

OFFICE OF NAVAL RESEARCH

GRANT N00014-89-J-1178

R&T Code 413q001-01

TECHNICAL REPORT NO. 26

Measurements and Modelling of Thin Silicon Dioxide Films on Silicon

by

A. Kalnitsky, S.P. Tay and J. P. Ellul  
Northern Telecom Electronics Ltd.  
185 Corkstown Rd. Nepean  
Ontario, Canada K2H 8V4

and

S. Chongsawangvirod, J.W. Andrews and E.A. Irene  
Department of Chemistry CB# 3290  
University of North Carolina  
Chapel Hill, NC 27599-3290

Submitted to the

The Journal of Electrochemical Society

AD-A207 853

DTIC  
ELECTROCHEMICAL SOCIETY  
MAY 15 1989  
S H D  
Cb

Reproduction in whole or in part is permitted for any purpose of the United States Government.

This document has been approved for public release and sale; its distribution is unlimited.

## REPORT DOCUMENTATION PAGE

<b>1a. REPORT SECURITY CLASSIFICATION</b> Unclassified		<b>1b. RESTRICTIVE MARKINGS</b>										
<b>2a. SECURITY CLASSIFICATION AUTHORITY</b>		<b>3. DISTRIBUTION/AVAILABILITY OF REPORT</b> Approved for public release; distribution unlimited.										
<b>2b. DECLASSIFICATION/DOWNGRADING SCHEDULE</b>												
<b>4. PERFORMING ORGANIZATION REPORT NUMBER(S)</b> Technical Report #26		<b>5. MONITORING ORGANIZATION REPORT NUMBER(S)</b>										
<b>6a. NAME OF PERFORMING ORGANIZATION</b> UNC Chemistry Dept.	<b>6r. OFFICE SYMBOL</b> <i>(If applicable)</i>	<b>7a. NAME OF MONITORING ORGANIZATION</b> Office of Naval Research (Code 413)										
<b>6c. ADDRESS (City, State and ZIP Code)</b> CB# 3290, Venable Hall University of North Carolina Chapel Hill, NC 27599-3290		<b>7b. ADDRESS (City, State and ZIP Code)</b> Chemistry Program 800 N. Quincy Street Arlington, Virginia 22217										
<b>8a. NAME OF FUNDING/SPONSORING ORGANIZATION</b> Office of Naval Research	<b>8b. OFFICE SYMBOL</b> <i>(If applicable)</i>	<b>9. PROCUREMENT INSTRUMENT IDENTIFICATION NUMBER</b> Grant #N00014-89-J-1178										
<b>8c. ADDRESS (City, State and ZIP Code)</b> Chemistry Program 800 N. Quincy Street Arlington, VA 22217		<b>10. SOURCE OF FUNDING NOS.</b> <table border="1" style="width: 100%; border-collapse: collapse; margin-top: 5px;"> <thead> <tr> <th style="width: 25%;">PROGRAM ELEMENT NO.</th> <th style="width: 25%;">PROJECT NO.</th> <th style="width: 25%;">TASK NO.</th> <th style="width: 25%;">WORK UNIT NO.</th> </tr> </thead> <tbody> <tr> <td> </td> <td> </td> <td> </td> <td> </td> </tr> </tbody> </table>		PROGRAM ELEMENT NO.	PROJECT NO.	TASK NO.	WORK UNIT NO.					
PROGRAM ELEMENT NO.	PROJECT NO.	TASK NO.	WORK UNIT NO.									
<b>11. TITLE (Include Security Classification)</b> MEASUREMENTS AND MODELLING OF THIN SILICON DIOXIDE FILMS ON SILICON												
<b>12. PERSONAL AUTHOR(S)</b> A. Kalnitsky, S.P. Tay, J.P. Ellul, S. Chongsawangvirod, J.W. Andrews and E.A. Irene												
<b>13a. TYPE OF REPORT</b> Interim Technical	<b>13b. TIME COVERED</b> FROM _____ TO _____	<b>14. DATE OF REPORT (Yr., Mo., Day)</b> May 9, 1989	<b>15. PAGE COUNT</b> 25									
<b>16. SUPPLEMENTARY NOTATION</b> The Journal of Electrochemical Society												
<b>17. COSATI CODES</b> <table border="1" style="width: 100%; border-collapse: collapse; margin-top: 5px;"> <thead> <tr> <th style="width: 33%;">FIELD</th> <th style="width: 33%;">GROUP</th> <th style="width: 33%;">SUB. GR.</th> </tr> </thead> <tbody> <tr> <td> </td> <td> </td> <td> </td> </tr> <tr> <td> </td> <td> </td> <td> </td> </tr> </tbody> </table>		FIELD	GROUP	SUB. GR.							<b>18. SUBJECT TERMS (Continue on reverse if necessary and identify by block number)</b>	
FIELD	GROUP	SUB. GR.										
<b>19. ABSTRACT (Continue on reverse if necessary and identify by block number)</b>  The ellipsometric measurement of refractive indices for films less than 50 nm thick is of dubious quality due to the significance of the size of random errors relative to the accuracy required to extract reliable index values from the measurements. In this study the various errors are quantitatively assessed as a function of the film thickness, and then compared with experimental data obtained from differently prepared silicon dioxide films on silicon. The new results confirm previous work that shows higher refractive indices for thinner films. Transmission electron microscopy results confirm the results and graded and discreet layer models are compared.												
<b>20. DISTRIBUTION/AVAILABILITY OF ABSTRACT</b> UNCLASSIFIED/UNLIMITED <input checked="" type="checkbox"/> SAME AS RPT. <input type="checkbox"/> DTIC USERS <input type="checkbox"/>		<b>21. ABSTRACT SECURITY CLASSIFICATION</b> Unclassified										
<b>22a. NAME OF RESPONSIBLE INDIVIDUAL</b> Dr. David L. Nelson		<b>22b. TELEPHONE NUMBER (Include Area Code)</b> (202) 696-4410	<b>22c. OFFICE SYMBOL</b>									

Measurements and Modelling of Thin Silicon Dioxide Films on Silicon

A. Kalnitsky, S.P. Tay and J.P. Ellul  
Northern Telecom Electronics Ltd.  
185 Corkstown Rd. Nepean  
Ontario, Canada K2H 8V4  
and

S. Chongsawangvirod, J.W. Andrews and E.A. Irene  
Department of Chemistry CB# 3290  
University of North Carolina  
Chapel Hill, NC 27599-3290

Abstract

The ellipsometric measurement of refractive indices for films less than 50 nm thick is of dubious quality due to the significance of the size of random errors relative to the accuracy required to extract reliable index values from the measurements. In this study the various errors are quantitatively assessed as a function of the film thickness, and then compared with experimental data obtained from differently prepared silicon dioxide films on silicon. The new results confirm previous work that shows higher refractive indices for thinner films. Transmission electron microscopy results confirm the results and graded and discreet layer models are compared.


Introduction

Present advanced silicon based devices use gate oxides less than 15 nm thick. There exists a number of crucial materials science issues associated with this very thin SiO<sub>2</sub> film regime. Firstly, there is no adequate Si oxidation

model that predicts the experimentally determined film thickness,  $L$ , versus oxidation time,  $t$ , although many attempts are reported in the literature (see for example discussions of this issue in refs 1 and 2). The most recent models (1,2) consider film stress near the Si-SiO<sub>2</sub> interface as an important element in dictating the kinetics of film growth and the properties of thin oxide film. These models describe an interfacial oxide that is both structurally and physically different from the SiO<sub>2</sub> that is further from the interface. Substantial recent experimental evidence exists that supports the contention that the oxide grown near the Si surface is indeed structurally (3,4) and physically different (5,6). Furthermore, based on ellipsometry measurements there are reports that the oxide near the interface is optically different yielding higher refractive indices than the SiO<sub>2</sub> further from the interface (7,8). This work included an optical model consisting of a thin interlayer oxide film having a considerably higher refractive index than pure SiO<sub>2</sub> interposed between the Si and SiO<sub>2</sub>. This model has been shown to explain the large measured indices for SiO<sub>2</sub> films less than 15 nm. If the presence of this interlayer film is ignored in the optical model, a gradual increase in the apparent refractive index of bulk SiO<sub>2</sub> film is obtained as the film thickness decreases. A recent transmission electron microscopy, TEM, study (9) has shown that the film thicknesses obtained for

SiO<sub>2</sub> films less than 10 nm correspond to ellipsometric thicknesses obtained using larger refractive indices than for thicker SiO<sub>2</sub> films. Of practical importance in thin film technology for SiO<sub>2</sub> films of less than 25 nm thick is that the measured difference in refractive index for the thin oxide films will significantly alter the resulting thickness calculated from the ellipsometry measurements. This is illustrated with the calculations in Table 1 where it is seen that if the larger refractive index of 1.6, as opposed to a typical bulk SiO<sub>2</sub> film value of 1.465 is used, a difference of more than 10% in oxide thickness will result, thereby affecting electric field calculations similarly.

While all of the reported findings and models appear quite plausible, it must be remembered that for films of nearly the same refractive index, the curves of the ellipsometric measurables,  $\Delta$ ,  $\Psi$ , as a function of film thickness converge as the film thickness decreases. As shown in Fig. 1, this convergence illustrates that the importance of the accuracy of the ellipsometric measurements grows larger for the very thin film refractive index measurements, because as the film gets thinner the constant experimental errors approach the magnitude of the observed changes in the refractive index. The usual iterative data reduction routines used to calculate film thickness and refractive index from the ellipsometric measurables,  $\Delta$  and  $\Psi$ , using a one film

Availability Codes	
Dist	Avail and/or Special
A-1	
	

optical model are typically constructed to return an effective thickness and/or refractive index value when the stability of the calculated values are within an arbitrary tolerance radius. Thus both the magnitude of the tolerance and the direction of approach to the tolerance circle (whether + or -) can bias the resulting calculated values. For example an iterative approach from the low side of the refractive index will result in a calculated index lower than the true value by the amount that the arbitrary error radius has on the index in the specific region of  $\Delta, \psi$  space for the calculation. Random search analysis routines obviate the directional bias problem, and are therefore used in the present study, but the effect of the magnitude of the tolerance radius is not eliminated, and this effect will be evaluated and shown below to be greater for thin  $\text{SiO}_2$  films.

In the present study we consider both the measurement and the data reduction errors resulting from ellipsometric measurements on very thin oxide films. We show that the measurements yield larger refractive indices for the very thin oxide films grown on Si, that are outside the usual errors found in ellipsometry. The thickness associated with the larger indices are in better agreement with transmission electron microscopy measurements of the oxide thicknesses. Finally, the higher indices for the very thin film are modeled according to an interlayer model and reasonable agreement is obtained between model and experiment with the

use of a graded refractive index interlayer as previously suggested (8,11).

#### Experimental Procedures

The ellipsometric measurements were made using a manual single wavelength ellipsometer in the polarizer, compensator, sample, analyzer, PCSA, configuration and using a laser light source at 632.8 nm. With divided circles capable of  $0.005^\circ$  resolution and frequently calibrated polarizing optics, the measurements of angles to  $0.01^\circ$  for the polarizer, analyzer and compensator is attainable. The angle of incidence is also obtained to about  $0.01^\circ$  based on autocollimation calibration of the optical bench. Two zone ellipsometric measurements are made in order to cancel systematic errors in the optical components (10). A set of calibration samples (thermal  $\text{SiO}_2$  grown on Si at various thicknesses from 7 to 120 nm) was used to check the consistency and reproducibility of the measurements after the frequent calibrations and throughout the course of this work. Based on these limits we estimate that  $\Delta$  and  $\Psi$  can be measured to about  $0.02^\circ$  and  $0.01^\circ$ , respectively.

A data reduction algorithm which virtually eliminates the effect of a tolerance radius is used in this study. This procedure assumes a non-absorbing layer of thin  $\text{SiO}_2$  film on Si substrate which for the case of  $\text{SiO}_2$  on Si using 632.8nm

light is a safe assumption. An iterative routine is used to find the solution for the real thickness and refractive index with the stringent demand of accuracy of  $10^{-6}$  in the refractive index and in the error radii of  $\Delta$  and  $\psi$ . Convergence is dictated by the localization of roots between two error values for  $\Delta$ ,  $\psi$  and the imaginary part of the thickness of opposite signs. While this algorithm begins with a preassigned value of refractive index which may give a biased calculated result, the negligible error in the real part of refractive index and thickness yields an almost "exact" solution. In later discussions we label the calculations that employ this algorithm as "exact", since the influence of the error radius is virtually eliminated.

Another recently published algorithm for ellipsometric data reduction (11) is based on the combination of random search and "regula falsi" procedures. This general purpose algorithm uses a randomly generated set of thickness,  $L$ , and refractive index,  $N_f$  values at the beginning of the solution process. New starting points for search are randomly regenerated every time the solution appears to diverge, leading to directionally un-biased calculated results. The two algorithms, based on different numerical procedures, were found to yield similar results.

The oxide films used in this study were grown or deposited on device quality lightly doped n and p type (100) oriented single crystal silicon wafers. The oxidations and



depositions were performed under various conditions to be reported below with the resulting data, and all using semiconductor grade gases and conventional wafer cleaning techniques. All the films used in this study were processed under conditions that yield device quality SiO<sub>2</sub> films. Ellipsometry measurements on various thickness from 10 to 120 nm were carried out by etch-back of the films toward the interface in a buffered HF solution (NH<sub>4</sub>F:HF/50:1).

### Results and Discussion

Two main types of error which can contribute to the scatter in the extracted refractive index values are truncation or round off error, and ellipsometer machine error. The round off error arises from truncating measured optical component values at the decimal position of reasonable certainty which is  $\pm 0.001$  for input values of  $\Delta$  and  $\psi$  for the thin film. The machine error arises from the precision to which the values of each optical component is known. Typical machine errors result in uncertainties of about  $\pm 0.01$  in  $\psi$  and  $\pm 0.02$  in  $\Delta$ . In order to assess the effect of these errors on the values of refractive index extracted from the measured  $\Delta, \psi$  values, a calculation is performed in which ideal values of  $\Delta$  and  $\psi$  are calculated for a transparent film with a refractive index of exactly 1.465 on a Si substrate. The wavelength assumed is 632.8 nm and the angle of incidence is 70.00°. From the calculated  $\Delta,$

$\psi$  values for film thicknesses, the above two  $\pm$  errors are then included one at a time. The "exact" algorithm is then applied to extract both film thickness and refractive index from the perturbed  $\Delta$ ,  $\psi$  values. Fig. 2a displays the results. Round off error within a tolerance radius of  $\Delta$  and  $\psi$  is  $\pm .005^\circ$ . The nearly horizontal dotted line includes the truncation error, but the error radius is nearly zero and so it is labeled as an "exact" calculation as was described above. Small random fluctuations in the calculated refractive index for films less than 5 nm are observed in this "exact" solution thereby confirming the random effects of the truncating process. It is seen that both the truncation error and the component error grow in importance as the film thicknesses decrease, thus rendering the extraction of refractive indices from the measured data increasingly difficult for thinner films, as was mentioned above. With the errors being random, the extracted values for refractive index should also scatter randomly around the true value, since the measured  $\Delta$ ,  $\psi$  values contain these errors. For an extracted value of refractive index to be considered different from 1.465, it must lie outside of these error curves. Hence from here on we will display the extracted index values against the error curve background shown in Fig 2a. Furthermore, errors in the angle of incidence,  $\phi$ , will also seriously affect the ellipsometric results (12). With our instrument calibrated frequently by

an autocollimation procedure, we estimate errors in  $\phi$  of less than  $\pm 0.01^\circ$ . Fig 2b shows this error evaluated similarly to 2a, and with the background of 2a included. We choose not to consider this error further in this study, because once the  $\phi$  is calibrated and set via the autocollimation procedure, the set value with any error is fixed for a series of measurements (i.e.  $\phi$  has either a + or - deviation from the true value) while the random errors inherent in each  $\Delta$ ,  $\psi$  measurement are included in a non systematic manner in each measurement as is the truncation error. Thus while the error in  $\phi$  will affect the absolute value of  $N_f$ , it will do so in a systematic manner for a series of measurements at one particular  $\phi$ , and will not contribute to the scatter in the measured values. During the course of the measurements taken in this study (more than a year)  $\phi$  was recalibrated at least several times. Fig. 3 shows a summary of refractive index values extracted from  $\text{SiO}_2$  samples that were prepared using a variety of experimental film preparation procedures. Before attempting to interpret the details of the processing effects, which will be discussed together with our proposed model, several important points are to be noticed. First, it is clear that the extracted refractive index values for all  $\text{SiO}_2$  films increase as the film thickness decreases, and that the values obtained are significant, since they are outside the error curves. At this point one might argue that the error

curves were calculated from error estimations that are too small. However, we believe that the error estimates for our frequently and carefully aligned instrument are both reasonable and conservative. Furthermore, we observe only positive deviations from the error curve bounds. Even if the considered errors were too small, the machine errors are random and therefore should result in random deviations for the extracted index. In fact for all the  $\text{SiO}_2$  films grown in this study, we observe only systematic positive deviations that grow as film thickness decreases. As mentioned above, the algorithms used for the refractive index calculation from the measurements, are all unbiased in the direction of convergence and all gave essentially the same results. Thus, we conclude that the increase in refractive index observed for thinner  $\text{SiO}_2$  films is real. This conclusion was reached by previous authors(7-9) in careful studies, but it was not clear from their earlier reports how the data and the errors compared.

With the apparent reality of higher refractive indices for the thin  $\text{SiO}_2$  films, concomitant errors must be made in the film thicknesses extracted from the data on the basis of the thick film refractive index. Simply put, the ellipsometric measurement of film thickness is essentially a measurement of the optical path length for the light through the film which is the product of the refractive index and the film thickness. Thus, if one chooses an erroneously low

refractive index, as would obtain for the common practice of using the thick  $\text{SiO}_2$  film refractive index, one would extract an erroneously large film thickness from the optical path length measurement, i.e. the ellipsometric measurement.

In order to further confirm this prediction, TEM measurements were performed on film substrate cross sections. Fig. 4 shows one such experiment and a comparison of the TEM and ellipsometric results for both the thick film and thin film refractive indices with respective film thicknesses are summarized in Table 2. The excellent agreement between the TEM and thicknesses obtained using the thin  $\text{SiO}_2$  film refractive index,  $N_f$ , values (the higher indices) confirms the thin film refractive index measurements and the systematically high thickness values obtained from the thick film indices is also supportive of the veracity of the thin film higher values for  $N_f$ .

For the purpose of optical modelling we shall adopt the phenomenological Si-SiO<sub>2</sub> interface model previously developed (1). According to this model higher density interfacial oxide undergoes a transition to bulk density dynamically in the process of film growth or high temperature anneal. The distance from Si-SiO<sub>2</sub> interface over which density relaxation takes place must be related to oxide viscosity at growth or anneal temperature. Since viscosity undergoes a transition at a viscous flow point (5,13,14) of approximately 950°C, the thickness of the high

density transition region should be minimized at higher temperatures and longer oxidation/anneal times. Our optical model of the interfacial region is based on a process-temperature dependent transition region width of approximately 3 nm, as suggested in (1). This notion also follows the thinking of Aspnes and Theeten that a realistic interface model should be based on a continuously graded structure (8).

We assume that oxide refractive index at any point is adequately approximated by the simple relationship:

$$n(x) = 2.44 \exp[-0.5 \cdot (X/S)^2] + 1.46 \quad (1)$$

where X is distance measured from the interface, and S is the process related parameter describing the transition region width. For the oxide thickness of zero, expression (1) gives a value close to the real part of silicon refractive index at 632.8 nm wavelength. Further away from the interface, the exponential term in (1) approaches zero and the refractive index assumes a customary nominal value of 1.46. For short distances, X, from the interface, equation (1) yields n(x) in the  $3.2 \pm 0.4$  range reported for the space-averaged interfacial oxide index (7, 8).

Film stratification for numerical analysis is illustrated in Figure 5. The structure is composed by successively adding arbitrarily thin layers to the film, starting with bare Si substrate. Each added layer of film is assumed to be homogeneous, with distance dependent refractive index value

assigned to it as shown in Figure 5. The thickness of this incremental layer, dictated by the speed and memory available on a computer in use, was set at 0.2 nm in our modelling exercise. The topmost layer of the structure is assigned  $N_f = 1.46$  when expression (1) yields  $n(x)=1.460001$ . Once this condition is met, the number of layers in the structure does not increase. Instead, the thickness of the last added layer is being incremented for modelling of films thicker than the transition region width. Simulated "iso-index" curves for  $N_f = 1.46$  and transition region width of 1.5 nm ( $S = 5$ ), 3.5 nm ( $S = 10$ ) and 5.5 nm ( $S = 15$ ) are plotted in Figure 6. A characteristic feature of the simulated iso-index plots, for structures with assumed transition region width, is movement of  $\psi$  to the left of the origin for very thin films. A similar effect is observed when the interfacial oxide is modelled as a discrete layer, as was done in reference (8); however, a discontinuity in the iso-index curve is seen to develop due to an abrupt transition from  $N_f = 3.2$  in the discrete transition layer to  $N_f = 1.46$  in the bulk. The iso-index curve for thicker films with an assumed transition region is seen to complete the first ellipsometric thickness period to the left of the origin and then follow the thin film curve (Figure 6), thus preserving the interfacial layer information in the subsequent ellipsometric periods.

We now take the simulated values of  $\Delta$ ,  $\psi$  for the graded

interface films and attempt to use these data with an algorithm, which treats the oxide layer as being homogeneous in index, to extract the refractive index and the film thickness values. The data set generated with  $S = 5$  (1.5 nm wide interface) and with  $S = 10$  (3.5 nm wide interface) were analysed by the algorithm (11). The results are summarized in Tables 3 and 4. Simulated data for wider transition region widths ( $S = 10$ ) give much stronger refractive index vs thickness dependence than narrow ( $S = 5$ ) transition region results. Extracted film thickness values are somewhat lower than the thickness values used to generate the  $\Delta$ ,  $\psi$  data.

It is instructive to compare the graded index model discussed above with a discreet interlayer model. As seen in Fig. 7 the graded index model with  $S = 15$  (5.5 nm wide graded interface) and the discreet layer model with a 2 nm layer with a 3.2 index both yield indistinguishable excellent fits to the data. The predicted abrupt behavior in  $\psi$  for the discreet layer model (as can be seen in Fig. 6) which would differentiate between the models cannot be observed within the accuracy of our ellipsometers. Also it is clear that other values for the adjustable parameters could yield good fits. Thus with the present hardware and available ellipsometric data the models are indistinguishable. However, at the present time, the graded interface model appears in better agreement with XPS and



stress studies (1,2) which indicate a gradual change from the interface to bulk structure.

From Fig. 3 it can be observed that the relative order for the measured refractive indices,  $N_f$ , for  $\text{SiO}_2$  films thicker than 30 nm agrees with a previous study (5) which shows a higher  $N_f$  with lower oxidation temperature. However, for films thinner than 30 nm there is no apparent order in  $N_f$  with oxidation temperature. At this time we offer no explanation but the larger scatter in the obtained  $N_f$  values for the thin films may be obscuring any trends in the data. Further work is required.

The PECVD  $\text{SiO}_2$  films that were deposited at about  $100^\circ\text{C}$  show a consistently thinner transition regime. Following from the graded index model, this may indicate that for the lower deposition temperatures there is less intermixing than with the thermally grown oxides.

#### Summary and Conclusions.

1. Sources of experimental errors, contributing to uncertainty in ellipsometric measurables,  $\Delta$ ,  $\psi$  are analysed. This analysis is extended to evaluate the maximum uncertainty in extracted refractive index values due to the limited accuracy of ellipsometric measurements.
2. Data reduction algorithms, suitable for thin film index extraction were reviewed. Thin films  $N_f$  values, extracted using these algorithms, are consistently higher than the

thick oxide value of 1.465. Comparison of thin film  $N_f$  against the "confidence limits" imposed on extracted index by our analysis allows the following conclusions to be reached:

a) observation of high index values is not an artifact of ellipsometric measurements or data reduction, but rather a reflection of physical phenomena in the film,

b) Simultaneous  $L$ ,  $N_f$  extraction yields a better estimate of film thickness than the fixed index analysis. This conclusion is supported by our ellipsometry vs TEM correlation.

3. A graded interface optical model is proposed to explain the process-dependent increase in index for thinner films. This model, while not unambiguous, is consistent with the observation of a high density transition region present at Si-SiO<sub>2</sub> interface, and qualitatively explains the experimentally observed dependence of refractive index on film thickness for different film growth conditions.

#### Acknowledgement.

The work was supported in part by Northern Telecom Electronics and the Office of Naval Research, ONR.

## References

1. F.J. Grunthaner and P.J. Grunthaner, *Materials Science Report*, Vol 1, No.2,3, December (1986).
2. E.A. Irene, *CRC Critical Reviews in Solid State and Materials Science*, 14, 175 (1988).
3. G. Lucovsky, M.J. Mantini, J.K. Srivastava and E.A. Irene, *J.Vac. Sci. Technol.B*, 5, 530 (1987).
4. G. Lucovsky, J.T. Fitch, E. Kobeda and E.A. Irene, *Proceedings of Electrochemical Society Meeting*, Atlanta, May (1988).
5. E.A. Irene, E. Tierney and J. Angillelo, *J. Electrochem. Soc.*, 129, 2594 (1982).
6. E. Kobeda and E.A. Irene, *J. Vac. Sci Technol. B*, 6, 574 (1988).
7. E.A. Taft and L. Cordes, *J. Electrochem. Soc.*, 126, 131 (1979).
8. D.E. Aspnes and J.B. Theeten, *J. Electrochem. Soc.*, 127, 1359 (1980).
9. N.M. Ravindra, J. Narayan, D. Fathy, J.K. Srivastava and E.A. Irene, *J. Mater.Res.*, 2, 216 (1987).
10. R.M.A. Azzam and N.M. Bashara, "Ellipsometry and Polarized Light", North Holland, 1977, Chap 5.
11. A. Kalnitsky, S.P. Tay and I.D. Calder, *J. Electrochem. Soc.*, 135, 1271 (1988).
12. D. Chandler-Horowitz, *Proc. Soc. Photo-Optical Instrum. Engrs.* 342, Integrated Circuit Metrology, 121 (1982)
13. E.P EerNisse, G.F. Derbenwick, *IEEE Trans. Nucl. Sci.* NS-23, 1534 (1976)
14. E.A. Irene, *J.Appl. Phys.*, 54, 5416 (1983)

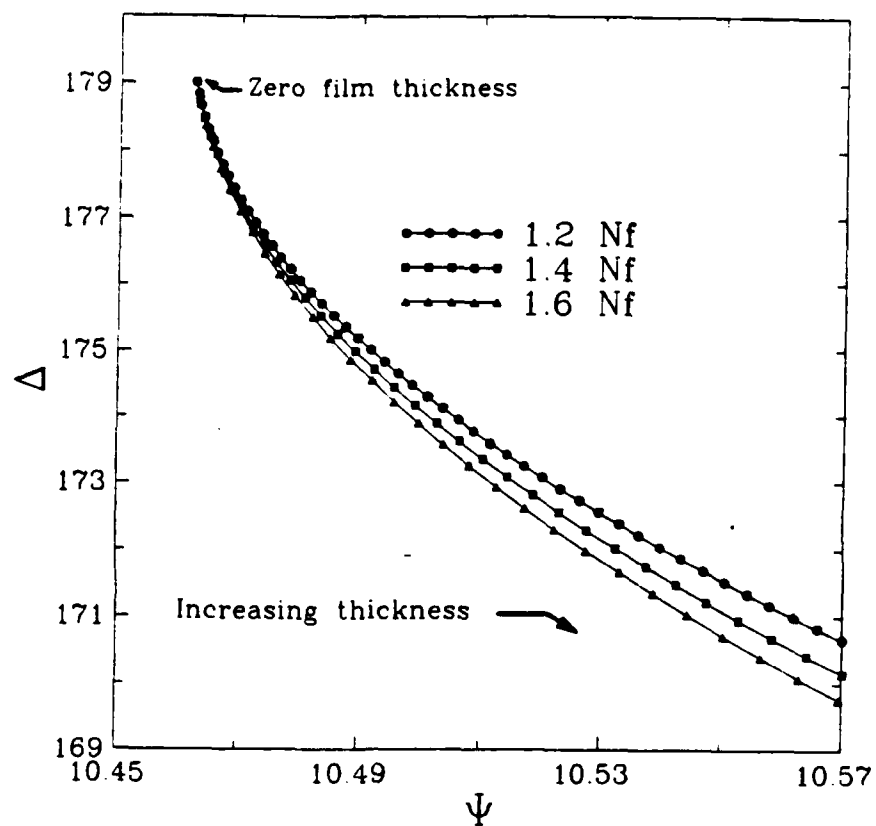


Figure 1. Theoretical plot of ellipsometric measurables,  $\Delta$ ,  $\Psi$ , as a function of film thickness (dots in .1 nm increments) for films with similar refractive indices.

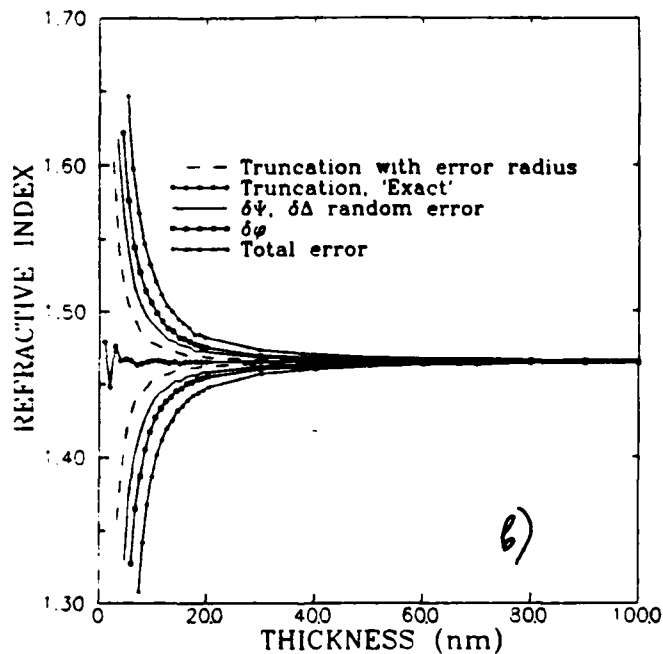
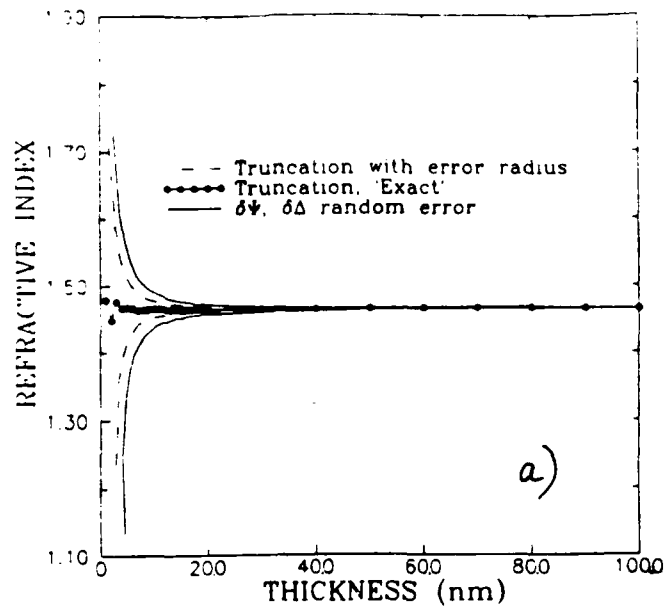


Figure 2. a) Theoretical assessment of truncation error with  $\pm .005$  error radius (dashed), truncation error of exact solution (connected dots), and  $\Delta, \psi$  error (continuous) arising from component error on a film with refractive index of 1.465 (horizontal) as a function of film thickness. b) Theoretical assessment of angle of incidence angle,  $\phi$ , error for a film with refractive index of 1.465 as a function of film thickness.

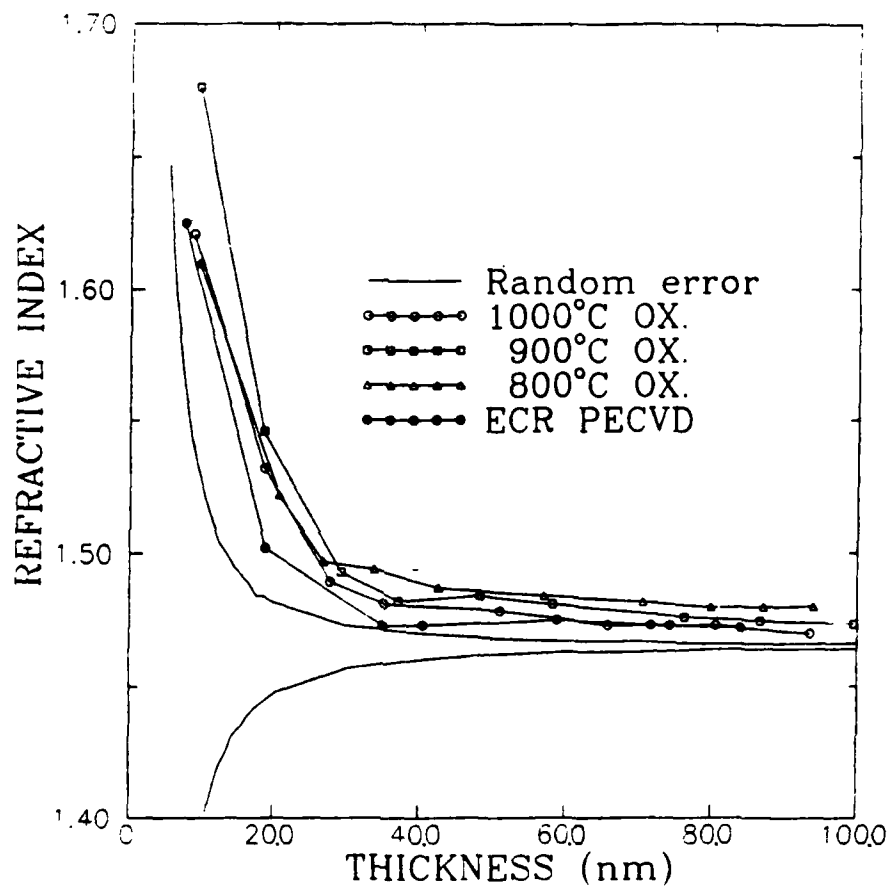


Figure 3. Experimental refractive index measurements on differently prepared films on a backdrop of the truncation and component errors (continuous line).

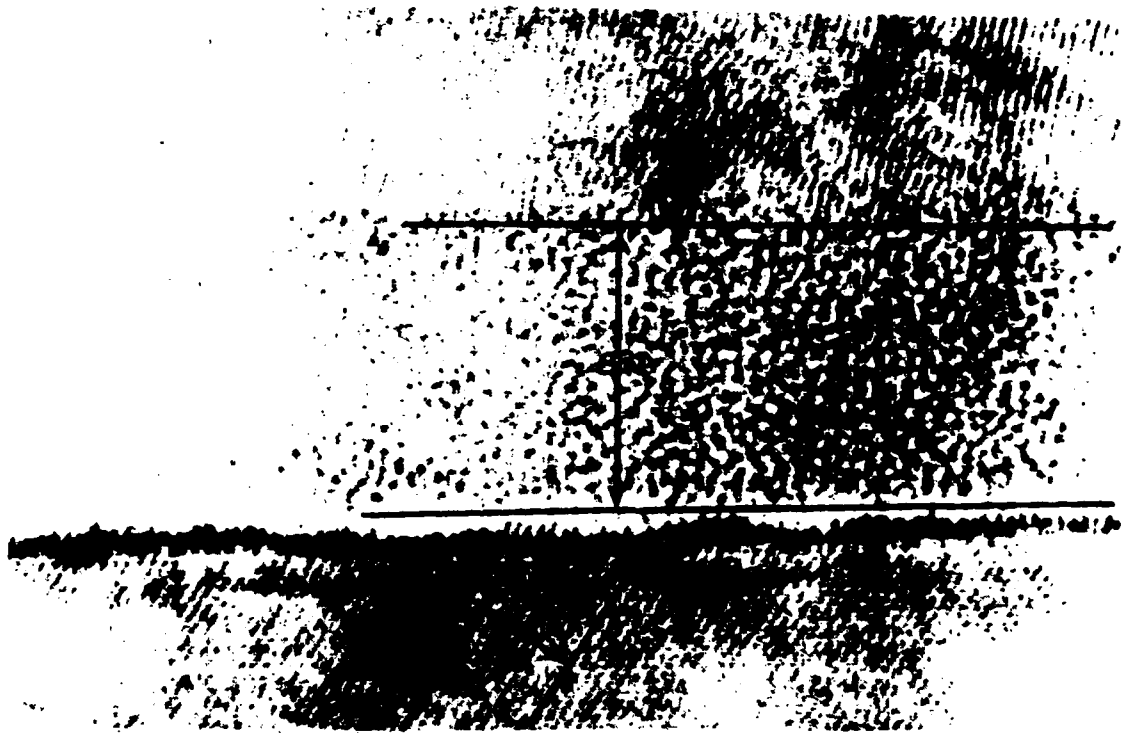


Figure 4. Transmission electron microscopy results of Si-SiO<sub>2</sub> crosssections showing SiO<sub>2</sub> film thicknesses.

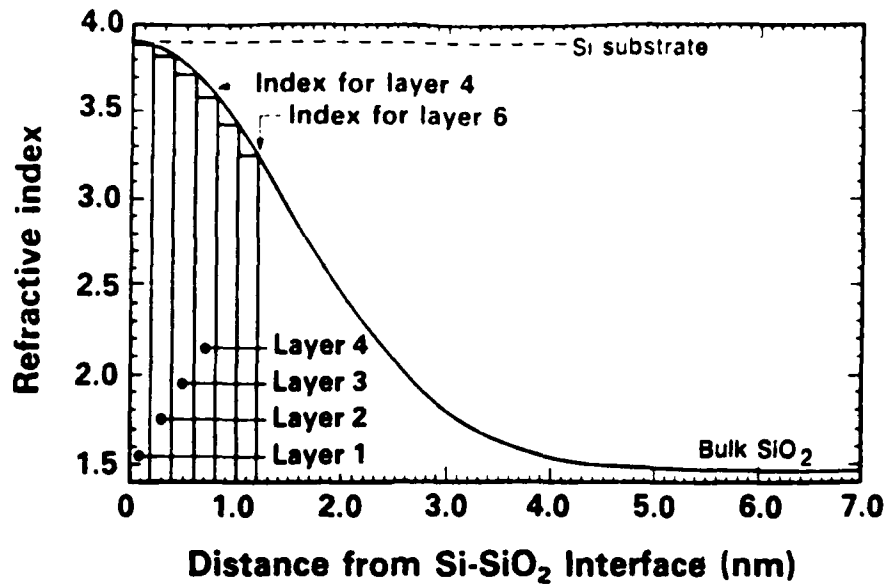


Figure 5. Stratification of  $\text{SiO}_2$  film: .2 nm wide layers are successively added to the structure until bulk value of refractive index is attained.

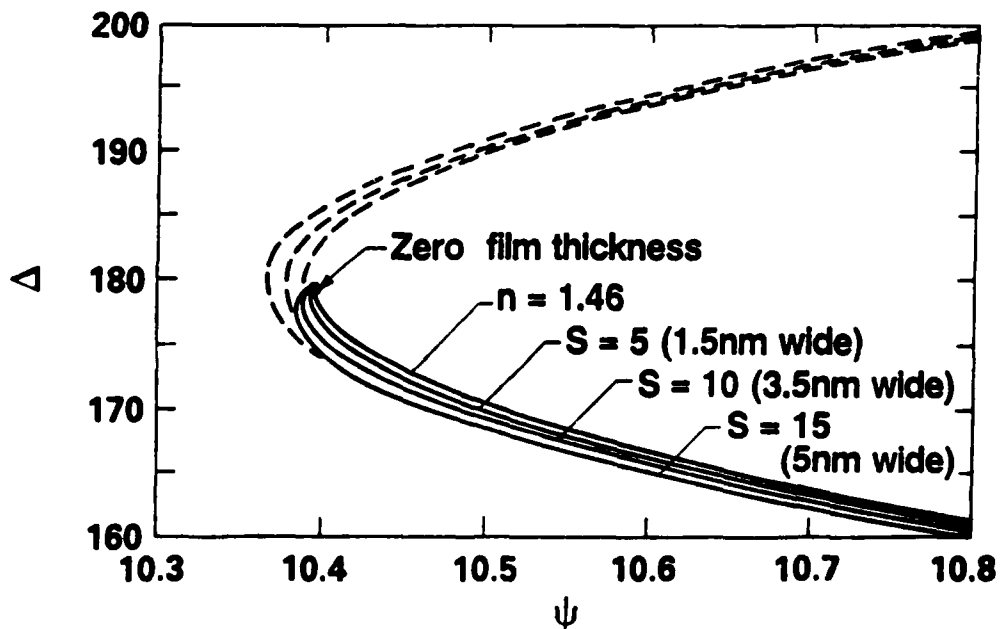


Figure 6. Computed 'iso-index' curves for thick oxide  $n=1.46$ , and for oxide with transition layer incorporated in the structure. Broken lines are for film thicknesses between 0.5 and 1.5 of the first ellipsometric period.



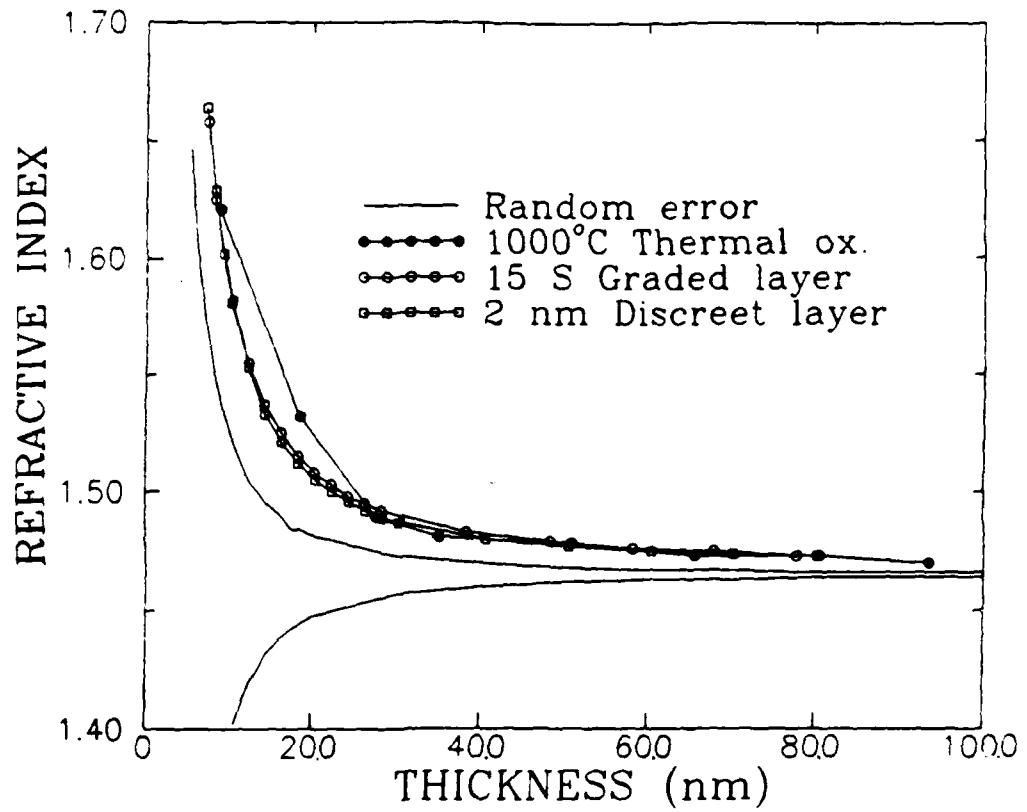


Figure 7. Comparison of extracted refractive index of simulated  $\Delta, \psi$  values of graded interlayer and discrete interlayer with experimental data.

**TABLE 1** Calculated effect of Refractive Index on Film Thickness

<u>Refractive index(N<sub>f</sub>)</u>	<u>%Δ in calculated film thickness</u>
1.265	37
1.365	13
1.465	0
1.565	-8
1.665	-12

$$\% \Delta = \frac{\text{Thickness using } N_f - \text{Thickness using } 1.465}{\text{Thickness using } 1.465}$$

**Table 2.** Comparison of film thicknesses obtained from ellipsometry using the thick film index, the thin film index and from TEM.

Sample	TEM (nm)	T(nm)	N <sub>f</sub>	T(nm) [N <sub>f</sub> =1.465]
1	11.±0.5	10.67	1.779	12.8
2	8.8	8.25	1.933	10.0
3	3.5	3.40	2.077	3.80

Table 3 Refractive index extraction from  $\Delta$ ,  $\Psi$  data simulated for narrow ( $S=5$ ) 1.5 nm transition layer.

L(nm)	Simulated values		Extracted $N_f$	Extracted L(nm)
	$\Delta$	$\Psi$		
0.0	179.252	10.3962	-	-
4.0	168.139	10.5407	1.733	3.3
8.0	157.169	10.9705	1.509	7.5
12.0	147.142	11.6419	1.489	11.5
16.0	138.224	12.5071	1.478	15.6
20.0	130.410	13.5178	1.474	19.6
24.0	123.596	14.6320	1.471	23.6
28.0	117.649	15.8157	1.469	27.6
32.0	112.437	17.0430	1.469	31.6
36.0	107.841	18.2949	1.467	35.6

Table 4 Refractive index extraction from  $\Delta$ ,  $\Psi$  data simulated for wide ( $S=10$ ) 3.5 nm transition layer.

L(nm)	Simulated values		Extracted $N_f$	Extracted L(nm)
	$\Delta$	$\Psi$		
0.0	179.252	10.3962	-	-
4.0	168.830	10.5096	1.912	2.995
8.0	157.797	10.9207	1.819	6.350
12.0	147.689	11.5767	1.639	10.200
16.0	138.687	12.4299	1.502	15.000
20.0	130.794	13.4318	1.493	19.020
24.0	123.912	14.5397	1.485	23.060
28.0	117.908	15.7190	1.481	27.060
32.0	112.645	16.9433	1.478	31.100
36.0	108.008	18.1931	1.476	35.100